Implementation of a diffuse interface method in a compressible multicomponent LES solver

Milan Pelletier, Schmitt Thomas, Sebastien Ducruix

Implementation of a diffuse interface method in a compressible multicomponent LES solver

M. Pelletier*, T. Schmitt, S. Ducruix
Laboratoire EM2C, CNRS, CentraleSupélec, Université Paris-Saclay, 3, rue Joliot Curie, 91192 Gif-sur-Yvette cedex, France
milan.pelletier@centralesupelec.fr and thomas.schmitt@centralesupelec.fr and sebastien.ducruix@centralesupelec.fr

Abstract

This study introduces a compressible diffuse interface method to simulate multicomponent flows for regimes ranging from subcritical two-phase flows to transcritical and supercritical flows. In the prospect of simulating a full cryogenic rocket-engine ignition, the model uses a real gas cubic equation of state to take advantage of its wide domain of validity. This choice requires a careful treatment in areas where the fluid state lies into the binodal region for subcritical regimes. In this respect, the model can be related to the family of multifluid methods such as Baer and Nunziato's 7-equation model (1986), considering velocity, pressure, temperature and chemical potential relaxations. Our objective is to restore hyperbolicity when an unstable state is encountered. To do so, a thermodynamic equilibrium is computed under a *one-fluid* hypothesis based on the Corresponding States Principle, yielding a two-phase stable fluid state. This relaxation process naturally impacts the dynamics in the areas where it happens and the subsequent consequences have been investigated. In particular, Jacobian matrices for the numerical schemes must be determined and adapted boundary conditions derivation must be provided. The method has been implemented into the unstructured solver AVBP, developed by CERFACS and IFPEN, and tested in a multidimensional flow in a subcritical regime. This allowed to observe the behavior of the model, especially in the two-phase regions.

1 Introduction

Many propulsion devices, such as liquid rocket engines (during ignition) or Diesel engines (during compression) operate over a wide range of chamber pressure. As a consequence, they are likely to involve thermodynamic states that can range from subcritical to supercritical conditions. In particular, transition from one regime to the other is encountered. The question of supercritical flows in combustion chambers has been and still is widely studied [1, 2, 3, 4]. Such flows require a description of the non-idealities in the molecular interactions, adressed by the Real-Gas (RG) thermodynamics. Among RG closures, cubic Equations of States (EoS), such as Van der Waals [5], Peng-Robinson [6] or Soave Redlich Kwong [7], have been deeply studied and prove to be relevant for supercritical simulations [8, 9, 10, 11, 12, 13]. However, in the subcritical domain, phase transitions occur and models are needed to handle both liquid-gas interfaces and atomization. Interface models can be split in two classes: Sharp Interface Methods (e.g. Level-Set [14, 15], Front-Tracking [16, 17] or Volume of Fluid [18]), representing the interface as a discontinuity and Diffuse Interface Methods (e.g. Multifluid Methods [19, 20, 21]), for which the interface is numerically represented as a diffuse region between pure phases. In the following, a diffuse interface approach is chosen as it offers a convenient framework for multicomponent compressible flows on unstructured grids. Also, as the interface is not explicitely tracked, the extension from subcritical two-phase flows to supercritical flows is expected to be more natural. The challenge here is then to blend the subcritical diffuse interface model with the supercritical-adapted cubic EoS to provide a description of the flow in the whole range of thermodynamic states encountered in industrial devices.

The objective of this work is to extend the use of cubic EoS to the subcritical regime. This is done by computing homogeneous equilibrium in the binodal region. This paper describes the extended thermodynamics in detail and its integration in a compressible solver.

The present paper is structured as follows: section 2 presents the flow model and the thermodynamic closure. In section 3, the derivation of important thermo-mechanical quantities will be presented, that allow the use of Taylor-Galerkin [22] numerical methods and Navier-Stokes Characteristic Boundary Conditions [23]. Eventually, in section 4, a two-dimensional test case is proposed to demonstrate the behavior of the method.

*Corresponding author: milan.pelletier@centralesupelec.fr

2 Flow Model

2.1 Diffuse Interface Model

The diffuse interface model considered here can be derived from the Baer and Nunziato's model [19] by assuming equilibria of velocity, temperature, pressure and chemical potentials. This allows to retrieve a 3-equation model, similar to Euler equations. A homogeneous equilibrium model is then obtained. It can be written as:

$$\frac{\partial \boldsymbol{U}}{\partial t} + \frac{\partial \mathcal{F}(\boldsymbol{U})}{\partial x} = 0, \tag{1}$$

where $\boldsymbol{U}$ and $\mathcal{F}(\boldsymbol{U})$ represent respectively the vector of conserved variables and their fluxes, given by:

$$\boldsymbol{U} = \left[\rho u, \quad \rho e_{\text{tot}}, \quad \rho Y_1, \quad \cdots \quad \rho Y_N\right]^T \tag{2}$$

$$\mathcal{F}(\boldsymbol{U}) = \left[\rho u^2 + P, \quad (\rho e_{\text{tot}} + P)u, \quad \rho Y_1 u, \quad \cdots \quad \rho Y_N u\right]^T. \tag{3}$$

The usual notations are used here, with ρ the density, Y_i the mass fraction of the i^{th} species, u the velocity, P the pressure and total specific energy $e_{\text{tot}} = e_s + e_c$, e_s being the sensible energy and $e_c = \frac{u^2}{2}$ the kinetic energy. This system of equations must be closed by an EoS.

2.2 Thermodynamic Closure

Among the possible choices, cubic EoS have proven to offer a good trade-off between simplicity, accuracy and ability to describe multicomponent mixtures [3, 24]. Such equations can be expressed as:

$$P = \frac{\rho r T}{1 - \rho b_m(\boldsymbol{Y})} - \frac{a_m(T, \boldsymbol{Y})\rho^2}{1 + \varepsilon_1 b_m(\boldsymbol{Y})\rho + \varepsilon_2 b_m^2(\boldsymbol{Y})\rho^2}, \tag{4}$$

with T the temperature, $\boldsymbol{Y} = \{Y_i\}_{i=1..N}$ the mixture composition, a_m and b_m the EoS mixture coefficients computed from Van der Waals mixing laws [24]. $r = \frac{R}{\overline{\text{W}}}$ denotes the specific gas constant of the mixture, R being the perfect gas constant, $\overline{\text{W}} = \left(\sum_{i=1}^{N} \frac{Y_i}{\text{W}_i}\right)^{-1}$ the mixture molar mass and $(\varepsilon_1, \varepsilon_2)$ the EoS parameters.

Here, a unique EoS is used for the description of liquid, vapour and supercritical states, similarly as [4]. Howevers, the formulation of the equilibrium problem is simplified assuming equality of species mass fraction in liquid and vapour phases (*one-fluid hypothesis*). This idea is motivated considering that the interface region in Diffuse Interface Models is an artificial mixture. The actual physical state of such region is locally not representative of the proper physical interface. The strategy considered here is then to avoid the full computation of the physical multicomponent equilibrium but rather compute the *one-fluid* equilibrium described hereafter, ensuring the preservation of the convexity of the EoS.

One-Fluid hypothesis: The equilibrium computation is performed assuming that the mixture species composition $\boldsymbol{Y}$ is *frozen* and *identical* for both liquid and gas phases, following a *one-fluid* hypothesis. Although the one-fluid treatment is widely used for cubic EoS in the one-phase or supercritical domain, it is used here in the case of two-phase flows, allowing to ensure the convexity of the EoS.

In the binodal region, as the one-phase fluid state is either metastable or unstable, the two-phase stable mixture is computed so that both phase have the same temperature, pressure and Gibbs free energy g, that is:

$$P_\ell = P_v = P, \qquad T_\ell = T_v = T, \qquad g_\ell = g_v = g, \tag{5}$$

respecting mixture density and specific sensible energy. Subscripts ℓ and v indicate respectively the liquid and vapour phases. The *one-fluid* hypothesis used here writes $\boldsymbol{Y} = \boldsymbol{Y}_\ell = \boldsymbol{Y}_v$.

The density and sensible energy of the fluid represent in this case mixture properties, with mixture defined using the liquid volume fraction α_ℓ:

$$\rho = \alpha_\ell \rho_\ell + (1 - \alpha_\ell)\rho_v \tag{6}$$

$$\rho e_s = \alpha_\ell \rho_\ell e_{s,\ell} + (1 - \alpha_\ell)\rho_v e_{s,v} \tag{7}$$

2.3 Practical implementation

Let ρ^p and e_s^p be the density and energy predicted by the numerical scheme. In the first place, the *one-phase* temperature T_m is determined finding the zero of function θ defined by:

$$\theta(\rho^p, T) = \frac{e_s^p - e_s^{\mathrm{EoS}}(\rho^p, T)}{e_s^p}, \tag{8}$$

where e_s^{EoS} is the sensible energy computed from the EoS.

Once this temperature is obtained, *one-phase* pressure is computed as $P_m = P^{\mathrm{EoS}}(\rho^p, T_m)$. The densities that satisfy the cubic EoS for the obtained (P_m, T_m) are computed from the EoS. If multiple roots are found, their fugacity is compared. The minimal fugacity solution being the stable one, the flow state is kept as single-phase if the predicted density is the one of minimal fugacity. Otherwise, a two-phase equilibrium must be computed. The computation of the *one-fluid* equilibrium is similar to that described in [25].

3 Mathematical Properties

This section aims at providing the derivation of the important mathematical properties of the Homogeneous Equilibrium Model. This is particularly interesting towards the implementation into the solver AVBP (see for example [26], for more details). AVBP is an unstructured compressible unsteady multicomponent solver jointly developed by CERFACS and IFPEN.

3.1 Jacobian Matrices

3.1.1 General Form

Among the numerical methods available in this solver, Two-Step Taylor-Galerkin methods (TTGC, TTG4A [22]) are particularly interesting as they provide a third-order convergence in space and time for a limited computational cost and a local stencil. Their derivation uses the so-called Cauchy-Kowalevski process, which requires to compute the Jacobian matrix of the flux (3), given by:

$$\boldsymbol{J}_{\mathcal{F}}(\boldsymbol{U}) = \left.\frac{\partial \mathcal{F}(\boldsymbol{U})_i}{\partial \boldsymbol{U}_j}\right|_{\boldsymbol{U}_{k,\ k\neq j}} = \begin{bmatrix} (2-b)u & b & -u^2+b(e_c-a_1) & \cdots & -u^2+b(e_c-a_N) \\ h_{\mathrm{tot}}-u^2 b & u(1+b) & \left[(e_c-a_1)b-h_{\mathrm{tot}}\right]u & \cdots & \left[(e_c-a_N)b-h_{\mathrm{tot}}\right]u \\ Y_1 & 0 & (1-Y_1)u & \cdots & -Y_N u \\ \vdots & & & \ddots & \\ Y_N & 0 & -Y_1 u & \cdots & (1-Y_N)u \end{bmatrix} \tag{9}$$

with coefficients $a_i = \left.\frac{\partial \rho e_s}{\partial \rho Y_i}\right|_{P,\rho Y_{j\neq i}}$ and $b = \left.\frac{\partial P}{\partial \rho e_s}\right|_{\rho, Y_j}$.

Expression (9) is valid for any thermodynamic closure. In the supercritical or one-phase domain, the usual form of the Jacobian matrix for cubic EoS naturally applies [23]. For points lying in the binodal region, as phase separation is considered by the equilibrium model, the derivation of differential relations at saturation is necessary.

3.1.2 Saturation derivatives and Clausius-Clapeyron relation for mixtures

In this respect, it is necessary to introduce *saturation derivatives*, which, for a thermodynamic quantity ψ usually expressed as a function of pressure, temperature and mixture composition, write:

$$\begin{cases} \left.\frac{\partial \psi}{\partial P}\right|_{\mathrm{sat},Y_i} = \left.\frac{\partial \psi}{\partial P}\right|_{T,Y_i} + \left.\frac{\partial \psi}{\partial T}\right|_{P} \vartheta_P & \text{(10a)} \\ \left.\frac{\partial \psi}{\partial Y_i}\right|_{\mathrm{sat},P,Y_{j\neq i}} = \left.\frac{\partial \psi}{\partial Y_i}\right|_{T,Y_{j\neq i}} + \left.\frac{\partial \psi}{\partial T}\right|_{P,Y_j} \vartheta_i & \text{(10b)} \end{cases}$$

where derivatives of temperature with respect to pressure and mixture composition, denoted respectively ϑ_P and ϑ_i at saturation follow the Clausius-Clapeyron relation [24], which formulation is extended here to multicomponent mixture under *one-fluid* equilibrium hypothesis. They read:

$$\vartheta_P = \left.\frac{\partial T}{\partial P}\right|_{\mathrm{sat},Y_j} = \frac{T(\rho_\ell - \rho_v)}{\rho_v \rho_\ell (h_{s,v} - h_{s,\ell})}; \qquad \vartheta_i = \left.\frac{\partial T}{\partial Y_i}\right|_{\mathrm{sat},Y_{j\neq i}} = \frac{g_{v,i} - g_{\ell,i}}{s_v - s_\ell} \tag{11}$$

with the partial Gibbs free in the vapor and liquid phases defined by $g_i = \left.\frac{\partial mg}{\partial m_i}\right|_{T,P,m_{j\neq i}}$ and evaluated respectively for $g_{v,i}$ at thermodynamic point $(T, \rho_v, \boldsymbol{Y})$ and for $g_{\ell,i}$ at $(T, \rho_\ell, \boldsymbol{Y})$.

3.1.3 Jacobian terms for two-phase equilibrium

Calculation of the terms a_i and b can be carried out by expressing the differential of the mixture volume sensible energy defined in (7) as follows:

$$\mathrm{d}\rho e_s = \alpha_\ell \,\mathrm{d}\big(\rho_\ell e_{s,\ell}\big) + (1-\alpha_\ell)\,\mathrm{d}\big(\rho_v e_{s,v}\big) + \big(\rho_\ell e_{s,\ell} - \rho_v e_{s,v}\big)\,\mathrm{d}\alpha_\ell \tag{12}$$

It is then worth mentioning that the single-phase quantities at equilibrium $\rho_\ell, \rho_v, e_{s,\ell}, e_{s,v}$ are function of the pressure and mixture composition only. For phase $\phi \in \{\ell, v\}$, volume-specific energy differential reads:

$$\mathrm{d}\big(\rho_\phi e_{s,\phi}\big) = \left.\frac{\partial \rho_\phi e_{s,\phi}}{\partial P}\right|_{\mathrm{sat},Y_j} \mathrm{d}P + \sum_{i=1}^{N} \left.\frac{\partial \rho_\phi e_{s,\phi}}{\partial Y_i}\right|_{\mathrm{sat},P,Y_{j\neq i}} \mathrm{d}Y_i \tag{13}$$

This expression can then be developped as:

$$\begin{aligned}\mathrm{d}\big(\rho_\phi e_{s,\phi}\big) = &\left[\rho_\phi\left(c_{p,\phi} - \alpha_\phi^T h_{s,\phi}\right)\vartheta_P + \rho_\phi \beta_\phi h_{s,\phi} - \alpha_\phi^T T\right]\mathrm{d}P \\ &+ \frac{\rho_\phi}{\rho}\sum_{i=1}^{N}\left[\left(c_{p,\phi} - \alpha_\phi^T h_{s,\phi}\right)\vartheta_i + e_{\phi,i} - \rho_\phi v_{\phi,i} e_{s,\phi}\right]\mathrm{d}(\rho Y_i)\end{aligned} \tag{14}$$

where $c_{p,\phi}$ is the specific heat capacity of phase ϕ, $\alpha_\phi^T = -\frac{1}{\rho_\phi}\left.\frac{\partial \rho_\phi}{\partial T}\right|_{P,Y_k}$ the thermal expansion coefficient, $\beta_\phi = \frac{1}{\rho_\phi}\left.\frac{\partial \rho_\phi}{\partial P}\right|_{T,Y_k}$ the isothermal compressibility coefficient, $h_{s,\phi} = e_{s,\phi} + \frac{P}{\rho_\phi}$ the sensible enthalpy and $v_{\phi,i}$ the partial specific volume of species i in phase ϕ.

Besides, the last term in equation (12) requires differentiating the liquid volume fraction, which can be done using (6):

$$\mathrm{d}\alpha_\ell = \mathrm{d}\left(\frac{\rho - \rho_v}{\rho_\ell - \rho_v}\right) = \frac{1}{\rho_\ell - \rho_v}\left[\mathrm{d}\rho - \alpha_\ell\,\mathrm{d}\rho_\ell - (1-\alpha_\ell)\,\mathrm{d}\rho_v\right] \tag{15}$$

which can be developed using (10) into:

$$\mathrm{d}\alpha_\ell = \tfrac{1}{\rho_\ell - \rho_v}\left[\left(\rho\alpha^T\right)_{\mathrm{mix}}\vartheta_P - (\rho\beta)_{\mathrm{mix}}\right]\mathrm{d}P + \tfrac{1}{\rho(\rho_\ell - \rho_v)}\sum_{i=1}^{N}\left[\left(\rho\alpha^T\right)_{\mathrm{mix}}\vartheta_i + \left(\rho^2 v_i\right)_{\mathrm{mix}}\right]\mathrm{d}(\rho Y_i), \tag{16}$$

where the subscript $_{\mathrm{mix}}$ for any quantity ψ denotes the mixture value $\psi_{\mathrm{mix}} = \alpha_\ell\psi_\ell + (1-\alpha_\ell)\psi_v$.

Using, at equilibrium, the equality $g_\ell = g_v$, one can write:

$$\frac{\rho_\ell e_{s,\ell} - \rho_v e_{s,v}}{\rho_\ell - \rho_v} = h_{s,\ell} - \frac{1}{\rho_\ell}\frac{T}{\vartheta_P} = h_v - \frac{1}{\rho_v}\frac{T}{\vartheta_P} = \alpha_\ell h_{s,\ell} + (1-\alpha_\ell)h_{s,v} - \alpha_\ell\frac{1}{\rho_\ell}\frac{T}{\vartheta_P} - (1-\alpha_\ell)\frac{1}{\rho_v}\frac{T}{\vartheta_P} \tag{17}$$

Finally, combining (17), (16) and (14), the mixture volume energy differential reads:

$$\begin{aligned}\mathrm{d}(\rho e_s) = &\left[\vartheta_P C_{p,\mathrm{mix}} - 2T\alpha^T{}_{\mathrm{mix}} + \frac{T}{\vartheta_P}\beta_{\mathrm{mix}}\right]\mathrm{d}P \\ &+ \frac{1}{\rho}\sum_{i=1}^{N}\left[\left(C_{p,\mathrm{mix}} - \frac{T}{\vartheta_P}\alpha^T{}_{\mathrm{mix}}\right)\vartheta_i + \left(P - \frac{T}{\vartheta_P}\right)(\rho v_i)_{\mathrm{mix}} + (\rho e_i)_{\mathrm{mix}}\right]\mathrm{d}(\rho Y_i).\end{aligned} \tag{18}$$

Then the calculation can be achieved by differentiating (7), which eventually yields:

$$a_i = \frac{1}{\rho}\left[\left(C_{p,\mathrm{mix}} - \frac{T}{\vartheta_P}\alpha^T{}_{\mathrm{mix}}\right)\vartheta_i + (\rho h_i)_{\mathrm{mix}} - \frac{T}{\vartheta_P}(\rho v_i)_{\mathrm{mix}}\right] \tag{19}$$

et

$$b = \frac{1}{\vartheta_P C_{p,\mathrm{mix}} - 2T\alpha^T{}_{\mathrm{mix}} + \frac{T}{\vartheta_P}\beta_{\mathrm{mix}}} \tag{20}$$

where $C_{p,\mathrm{mix}} = \alpha_\ell\rho_\ell c_{p,\ell} + (1-\alpha_\ell)\rho_v c_{p,v}$ is the mixture volume-specific isobaric heat capacity, $\alpha^T_{\mathrm{mix}} = \alpha_\ell\alpha_\ell^T + (1-\alpha_\ell)\alpha_v^T$ is a mixture thermal expansion coefficient and $\beta_{\mathrm{mix}} = \alpha_\ell\beta_\ell + (1-\alpha_\ell)\beta_v$ a mixture isothermal compressibility coefficient. In these expressions, for each phase $\phi \in \{\ell, v\}$ appear the thermal expansion and isothermal compressibility coefficients and the specific isobaric heat capacity $c_{p,\phi} = \left.\frac{\partial h_{s,\phi}}{\partial T}\right|_P$.

3.2 Speed of Sound and Characteristic Boundary Conditions

Once the Jacobian matrix has been calculated, its diagonalization gives access to important mathematical properties of the model. This allows to compute the speed of sound to verify the hyperbolicity of the PDE and also to derive the so-called Characteristic Boundary Conditions introduced by Poinsot and Lele [23].

3.2.1 Jacobian Matrix for Primitive variables and Speed of Sound

In the first place, it is helpful to write system (1) in its non-conservative pseudo-linearized form, in terms of primitive variables $\boldsymbol{V} = (u, P, \rho Y_1, ..., \rho Y_N)^T$. This reads:

$$\frac{\partial \boldsymbol{V}}{\partial t} + \boldsymbol{J}^p_{\mathcal{F}}(\boldsymbol{V}) \frac{\partial \boldsymbol{V}}{\partial x} = 0, \tag{21}$$

with the Jacobian matrix expressed this time in primitive variables:

$$\boldsymbol{J}^p_{\mathcal{F}}(\boldsymbol{V}) = \begin{bmatrix} u & \rho^{-1} & 0 & 0 & \cdots & 0 \\ \rho b\left(h_s - \sum_{i=1}^N Y_i a_i\right) & u & 0 & 0 & \cdots & 0 \\ \rho Y_1 & 0 & u & 0 & \cdots & 0 \\ \rho Y_2 & 0 & 0 & \ddots & & 0 \\ \vdots & \vdots & \vdots & & \ddots & \vdots \\ \rho Y_N & 0 & 0 & \cdots & 0 & u \end{bmatrix}. \tag{22}$$

This form once again stands for any thermodynamic closure. h_s here indicates the specific sensible enthalpy $h_s = e_s + P/\rho$. The term $c^2 = b\left(h_s - \sum_{i=1}^N Y_i a_i\right)$, can be expressed under the form:

$$c^2 = b\left(h_s - \sum_{i=1}^N Y_i a_i\right) = \frac{P}{\rho^2}\left.\frac{\partial P}{\partial e_s}\right|_{s,Y_j} - \frac{P}{\rho^2}\left.\frac{\partial \rho}{\partial e_s}\right|_{s,Y_j}\left.\frac{\partial P}{\partial \rho}\right|_{e_s,Y_j} + \sum_{i=1}^N Y_i \left.\frac{\partial P}{\partial \rho Y_i}\right|_{e_s,\rho Y_{j\neq i}}, \tag{23}$$

where s is the specific entropy of the two-phase mixture. It can be shown that this definition reduces to the classical speed of sound definition for the two-phase *one-fluid* equilibrium. Finally, the usual form of the Jacobian matrix in primitive variables remains valid for the two-phase mixture:

$$\boldsymbol{J}^p_{\mathcal{F}}(\boldsymbol{V}) = \begin{bmatrix} u & \rho^{-1} & 0 & \cdots & 0 \\ \rho c^2 & u & 0 & \cdots & 0 \\ \rho Y_1 & 0 & \ddots & & \vdots \\ \vdots & \vdots & & \ddots & 0 \\ \rho Y_N & 0 & \cdots & 0 & u \end{bmatrix} \quad ; \quad c = \sqrt{\left.\frac{\partial P}{\partial \rho}\right|_s}, \tag{24}$$

and the speed of sound appears to have the usual definition, except that ρ and s are, in the binodal region, variables of the two-phase mixture at equilibrium. The mixing law for specific entropy is:

$$\rho s = \alpha_\ell \rho_\ell s_\ell + (1 - \alpha_\ell)\rho_v s_v. \tag{25}$$

The calculation of the speed of sound in the two-phase case can be achieved by expressing the differential of specific entropy from density and pressure differentials. These developments provide the following form for the speed of sound to the square:

$$c^2 = \left[\rho\left(\frac{1}{\beta_{\text{mix}}}\left(\beta_{\text{mix}} - \alpha^T_{\text{mix}}\vartheta_P\right)^2 + \frac{C_{v,\text{mix}}}{T}\vartheta_P^2\right)\right]^{-1} \tag{26}$$

which remains positive as a combination of positive quantities. The system's hyperbolicity is then preserved.

3.2.2 Characteristic Boundary Conditions

Diagonalization of the Jacobian $\boldsymbol{J}^p_{\mathcal{F}}(\boldsymbol{V})$ yields the so-called characteristic form. The characteristic Jacobian Matrix $\boldsymbol{J}^c_{\mathcal{F}}(\boldsymbol{W})$ can be expressed using transformation matrices $\boldsymbol{L_U} = \boldsymbol{R_U}^{-1}$ as:

$$\boldsymbol{J}^c_{\mathcal{F}}(\boldsymbol{W}) = \boldsymbol{L_U}\boldsymbol{J}_{\mathcal{F}}(\boldsymbol{U})\boldsymbol{R_U}, \tag{27}$$

these transformation matrices allowing to change basis between conservative and characteristic variables:

$$\begin{cases} \partial \boldsymbol{W} = \boldsymbol{L_U} \partial \boldsymbol{U}, & \text{(28a)} \\ \partial \boldsymbol{U} = \boldsymbol{R_U} \partial \boldsymbol{W}. & \text{(28b)} \end{cases}$$

As a consequence of $\boldsymbol{J}^p_{\mathcal{F}}(\boldsymbol{V})$ taking the usual form despite the two phase closure, its diagonalized form remains similar to its one-phase counterpart, as diagonalization yields:

$$\boldsymbol{J}^c_{\mathcal{F}}(\boldsymbol{W}) = \begin{bmatrix} u+c & 0 & \cdots & \cdots & 0 \\ 0 & u-c & \ddots & & \vdots \\ \vdots & \ddots & u & \ddots & \vdots \\ \vdots & & \ddots & \ddots & 0 \\ 0 & \cdots & \cdots & 0 & u \end{bmatrix} \tag{29}$$

$$\boldsymbol{L_U} = \frac{b}{\rho c} \begin{bmatrix} -(u+\frac{c}{b}) & 1 & (e_c-a_1)+\frac{c}{b}u & \cdots & (e_c-a_N)+\frac{c}{b}u \\ -(u-\frac{c}{b}) & 1 & (e_c-a_1)-\frac{c}{b}u & \cdots & (e_c-a_N)-\frac{c}{b}u \\ \frac{\rho u}{c}Y_1 & -\frac{\rho}{c} & \frac{\rho c}{b}-\frac{(e_c-a_1)\rho Y_1}{c} & \cdots & -\frac{(e_c-a_1)\rho Y_N}{c} \\ \vdots & \vdots & \vdots & \ddots & \vdots \\ \frac{\rho u}{c}Y_N & -\frac{\rho}{c} & -\frac{(e_c-a_1)\rho Y_N}{c} & \cdots & \frac{\rho c}{b}-\frac{(e_c-a_N)\rho Y_N}{c} \end{bmatrix}, \tag{30a}$$

$$\boldsymbol{R_U} = \begin{bmatrix} \frac{\rho}{2c}(u+c) & \frac{\rho}{2c}(u-c) & u & \cdots & u \\ \frac{\rho}{2c}\left(e_c+cu+\frac{c^2}{b}-\overline{a}\right) & \frac{\rho}{2c}\left(e_c-cu+\frac{c^2}{b}-\overline{a}\right) & \frac{e_c}{b}-a_1 & \cdots & \frac{e_c}{b}-a_N \\ \frac{\rho Y_1}{2c} & \frac{\rho Y_1}{2c} & 1 & \cdots & 0 \\ \vdots & \vdots & \vdots & \ddots & \vdots \\ \frac{\rho Y_N}{2c} & \frac{\rho Y_N}{2c} & 0 & \cdots & 1 \end{bmatrix}. \tag{30b}$$

with $\overline{a} = \sum_{i=1}^{N} Y_i a_i$ One observes that the modifications needed to write the Characteristic Boundary Conditions in the two-phase case reduce to modifying thermodynamic coefficients a_i, b and c (the speed of sound), according to (19), (20) and (26). Several validations for these results may be found in [25]. Here, a demonstrating case is proposed to observe the behaviour of the homogeneous equilibrium model in a realistic case.

4 Cryogenic Methane/Oxygen Coaxial Injection in 2D

Validations of the derivations given above are described in the one-component case in [25]. Equivalent results are found for the model in the case of multicomponent mixtures. In order to test the model, a cryogenic coaxial injection of liquid oxygen (LOx) and Methane is computed.

Case Description: In this computation, the central stream is pure LOx with density $\rho_{O_2} = 1050$ kg/m^3 and velocity $v_{O_2} = 10$ m/s. Peripheral streams are pure vapour CH_4 at $\rho_{CH_4} = 10$ kg/m^3 and velocity $v_{CH_4} = 150$ m/s. Pressure is set to 10 bar in the chamber.

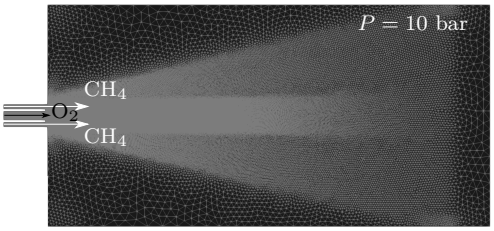

Figure 1: Computation Details

Numerical Setup: The unstructured mesh contains 50×10^3 nodes, as displayed in Figure 1. The solver is AVBP, using the two-step Taylor-Galerkin scheme TTG4A (see [22]) with the adapted Jacobian matrices described previously.

Results: Density field snapshots are shown in Figure 2. The dynamics are similar to supercritical mixing since no surface tension model is used at the moment. Still, the density gradient is noticeably strong and well handled by the solver. Figure 3 displays the two-phase region, which appears to be diffused over the domain as no interface sharpening method is used here.

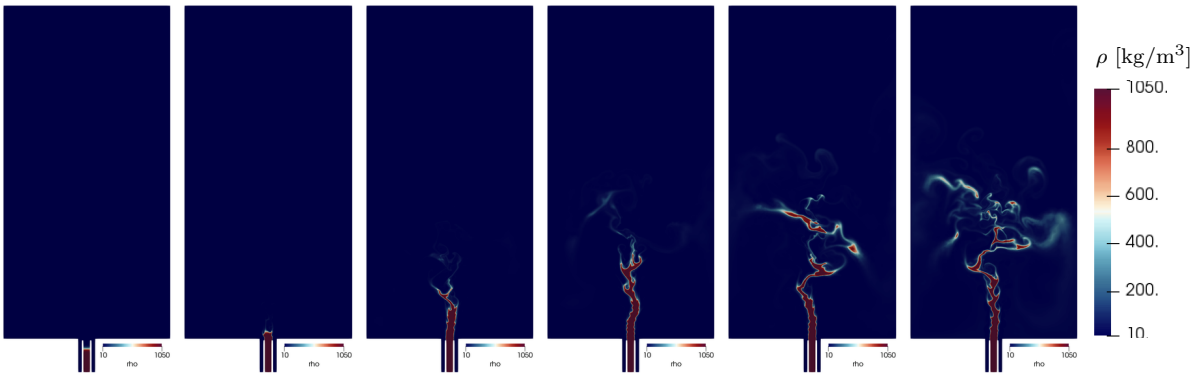

(a) $t = 0$ s (b) $t = 1.9$ ms (c) $t = 3.8$ ms (d) $t = 5.7$ ms (e) $t = 7.6$ ms (f) $t = 9.5$ ms

Figure 2: Snapshots of the density field. Values span from 10 kg/m^3 to 1050 kg/m^3

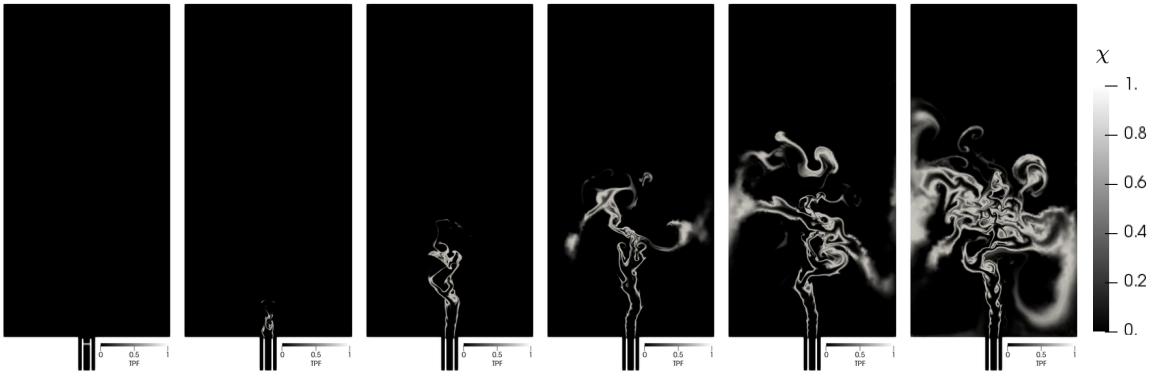

(a) $t = 0$ s (b) $t = 1.9$ ms (c) $t = 3.8$ ms (d) $t = 5.7$ ms (e) $t = 7.6$ ms (f) $t = 9.5$ ms

Figure 3: two-phase flow marker: $\chi = 4\alpha_\ell(1 - \alpha_\ell)$, so that $\chi \in [0, 1]$.

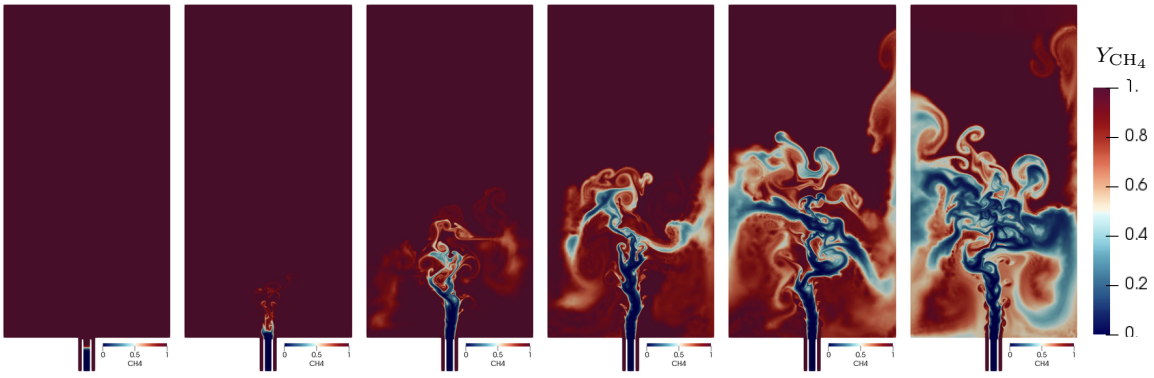

(a) $t = 0$ s (b) $t = 1.9$ ms (c) $t = 3.8$ ms (d) $t = 5.7$ ms (e) $t = 7.6$ ms (f) $t = 9.5$ ms

Figure 4: Snapshots of the methane mass fraction field. $Y_{\mathrm{CH_4}} \in [0, 1]$

5 Conclusion and Future Work

The present article details a simplified version of the Homogeneous Equilibrium Method to extend the use of Cubic EoS to subcritical regimes. The practical implementation of the equilibrium computation has been described and the mathematical properties have been investigated, to provide the flow model's Jacobian matrix together with its corresponding Characteristic Boundary Conditions implementation. In particular, it has been observed that the form of the resulting flow model is similar to the usual one-phase case. In addition, a multicomponent coaxial injection test case is computed, showing encouraging results.

Current developments focus on the implementation of a surface tension model which is the next step towards the development of a solver able to handle the whole range of pressure encountered in industrial combustors such as rocket and Diesel engines. In addition, interface sharpening methods are investigated to prevent unphysical diffusion of the interface area.

6 Acknowledgements

The authors acknowledge funding from ANR through project ANR-14-CE22-0014 (SubSuperJet)

References

[1] Candel, S., Juniper, M., Singla, G., Scouflaire, P. and Rolon, C. *Combustion Science and Technology* **178**, 161–192 (2006).

[2] Müller, H., Niedermeier, C. A., Matheis, J., Pfitzner, M. and Hickel, S. *Physics of Fluids* **28**, 015102 (2016).

[3] Yang, V. *Proceedings of the Combustion Institute* **28**, 925–942 (2000).

[4] Matheis, J. and Hickel, S. *International Journal of Multiphase Flow* **99**, 294 – 311 (2018).

[5] van der Waals, J. D. *Journal of Statistical Physics* **20**, 200–244 (1979).

[6] Peng, D.-Y. and Robinson, D. B. *Indust. & Engineering Chemistry Fundamentals* **15**, 59–64 (1976).

[7] Soave, G. *Chemical Engineering Science* **27**, 1197 – 1203 (1972).

[8] Oefelein, J. C. *Combustion Science and Technology* **178**, 229–252 (2006).

[9] Urbano, A. *et al. Combustion and Flame* **169**, pp. 129–140 (2016).

[10] Hakim, L. *et al. Proceedings of the Combustion Institute* **35**, 1461 – 1468 (2015).

[11] Schmitt, T., Selle, L., Ruiz, A. and Cuenot, B. *AIAA journal* **48**, 2133–2144 (2010).

[12] Schmitt, T., Méry, Y., Boileau, M. and Candel, S. *Proceedings of the Combustion Institute* **33**, 1383–1390 (2011).

[13] Zong, N. and Yang, V. *Combustion Science and Technology* **178**, 193–227 (2006).

[14] Osher, S. J. *Journal of Computational Physics* **79**, 1–5 (1988).

[15] Desjardins, O., Moureau, V. and Pitsch, H. *Journal of Computational Physics* **227**, 8395 – 8416 (2008).

[16] Glimm, J. *et al. SIAM Journal on Scientific Computing* **19**, 703–727 (1998).

[17] Terashima, H. and Tryggvason, G. *Journal of Computational Physics* **228**, 4012 – 4037 (2009).

[18] Hirt, C. and Nichols, B. *Journal of Computational Physics* **39**, 201 – 225 (1981).

[19] Baer, M. and Nunziato, J. *International Journal of Multiphase Flow* **12**, 861 – 889 (1986).

[20] Perigaud, G. and Saurel, R. *Journal of Computational Physics* **209**, 139–178 (2005).

[21] Kapila, A. K., Menikoff, R., Bdzil, J. B., Son, S. F. and Stewart, D. S. *Physics of Fluids* **13**, 3002–3024 (2001).

[22] Colin, O. and Rudgyard, M. *Journal of Computational Physics* 338–371.

[23] Poinsot, T. J. and Lele, S. K. *Journal of Computational Physics* **101**, 104–129 (1992).

[24] Poling, B. E. and Prausnitz, J. M. *the Properties of Gases and Liquids,* McGraw–Hill (2001).

[25] Pelletier, M., Nayigizente, D., Schmitt, T. and Ducruix, S. *INCA Conference* (2017).

[26] Moureau, V. *et al. Journal of Computational Physics* **202**, 710–736 (2005).